

ON THE RELATIONSHIP BETWEEN OPTICAL AND STRUCTURAL PROPERTIES OF POLYMER FILMS MODIFIED BY CARBON MICRO AND NANOPARTICLES

Tamara KOVALEVSKAYA*, Mikhail IHNATOUSKI*, Anatoly SVIRIDENOK*, Sergey ZHDANOK**,
Andrey KRAUKLIS**, Vladimir VOINA***, Andrey STEPURO****

*Research Center of Resource Saving Problems of National Academy of Sciences of Belarus, Tizenhauza sq., 7, Grodno, 230023 Republic of Belarus, Tel.: +375-152-720100, +375-152-738185

**A.V.Lykov Institute of Heat and Mass Transfer of National Academy of Sciences of Belarus, P. Brovka Str., 15, Minsk, BY-220072, Republic of Belarus

***Yanka Kupala Grodno State University, Ozeshko str., 22, 230023 Grodno, Republic of Belarus

****Institute Of Pharmacology and Biochemistry of National Academy of Sciences of Belarus, Grodno Branch: 50 Leninskaga Kamsamola Boulevard, Grodno BY-230017, Republic of Belarus

mii_by@mail.ru, office@itmo.by, krauklis@itmo.by, biophys@biochem.unibel.by

Abstract: The studies were concentrated on investigations of optical and structural characteristics of polymeric films filled by carbon micro and nanoparticles. Light transmission in the region of visible spectra of the films based on gelatin and polyvinyl alcohol was found to be almost independent of the wavelength. Carbon particles appeared to have no intrinsic absorption bands within the UV region. In the case of aggregation, nanotubes start to form clusters with an optical fractal structure, while the films display spatial fluctuations in transparency accompanied by deviations from the Bourguier-Lambert-Beer law. In contrast to nanoparticles, microparticles reduce the roentgen level of crystallinity of the films.

1. INTRODUCTION

Organic polymers and composite materials on their base have found extensive application in optical industry nowadays (lens, filter, screen, waveguide, car glass, etc.). Still new vistas have appeared lately thanks to the development and application of carbon nanoparticles in the composition of optical materials. Fine size, great specific surface and opacity of carbon nanoparticles in the UV and visible spectrum impart specific optical properties to nanocomposites (Du et al., 2006; Ajayan et al., 2003; Harris, 2003; Pool-jr and Owens, 2006; Kovalevskaya et al., 2006, 2007). It should be noted that the dependence of spectral characteristics on the type of nanoparticles (dimensions, shape, production process, surface treatment), as well as composition, structure of the polymeric matrix and technological procedures used have been scarcely examined as yet.

The aim of the present work was to study optical and structural peculiarities of polymeric films filled by carbon micro and nanoparticles with a modified atomic lattice structure.

2. MATERIALS AND RESEARCH METHODS

Microsized graphite particles (Gr) and ultradispersed nanomaterials (UNT) were employed to modify the polymer. The powder of UNT1 contained up to 30 mass% of multiwalled nanotubes and UNT2 - more than 60 mass%.

The composite films based on polyvinyl alcohol (PVA) and gelatin (Ge) were obtained by pouring aqua dispersion of a mixture of the polymeric powder and carbon fillers

onto the surface of monocrystalline silicon (Si) or glass wafers. The films of 30-50 μm thickness were produced by pouring on Si and 60-140 μm thick – on glass. The films based on polyamide 6 (PA) were manufactured by molding composite granules under a glass transition temperature. The characteristics of the samples are presented in Table 1.

The transmission spectra $T(\lambda)$ and the optical density spectra $D(\lambda)$ in the UV and visible wavelength range λ were recorded using spectrophotometers Specord-M40 and Specord-M500. X-ray patterns were obtained using a diffractometer DRON-2,0 with radiation CuK_α filtered to $\lambda = 0.1542$. The microimages of the films in the transmitted light were obtained by an optical microscope Micro-200T equipped with a digital video camera.

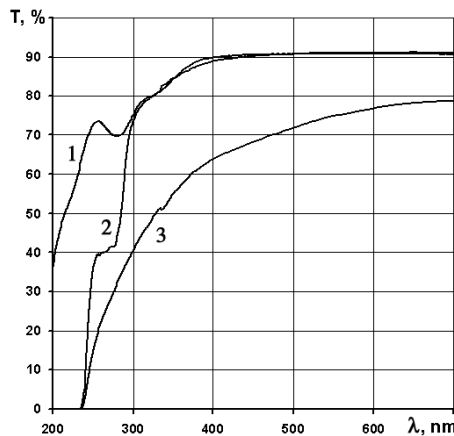
Tab. 1. Composite films, their composition and substrate used at preparation

Sample No.	Matrix	Filler	Substrate
f1	PVA	—	glass
f2	Ge	—	Si
f3	Ge	Graphite	Si
f4	PVA	Graphite	glass
f5	PVA	Graphite	Si
f6	PVA	UNT2	glass
f7	PVA	UNT1	glass
f8	PA	—	Al
f9	PA	UNT2	Al

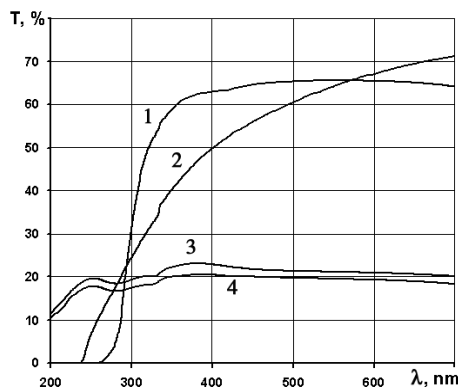
3. RESULTS AND DISCUSSION

3.1. Optical properties of the films

Most typical transmission spectra for unfilled films are illustrated in Fig. 1a. It is evident that PA films are less transparent and do not contain any weak absorption bands on the background of a gradual transmission (T) growth with increasing wavelength (λ). It has been proved earlier (Kovalevskaya et al., 2006) that a strong light weakening in these films in the 200÷400 nm region is attributed to Reyleigh's scattering. We have also observed domination of Reyleigh's scattering in the UV spectra of PVA and Ge films whose value is proportional to λ^{-4} , which is known to be characteristic of the optically inhomogeneous media with density fluctuations and fine foreign particle inclusions. Light scattering in the polymers may also take place on the residual stresses (Kawasaki and Kuwana, 2000), which are most likely to occur in PA-based films manufactured by hot molding. This is, probably, the reason, why the scattering takes place in them at a higher λ than in PVA and Ge.



a)



b)

Fig. 1. Transmission spectra: a) of unfilled films: 1 – PVA (f1); 2 – Ge (f2); 3- PA (f8); b) of films filled by: 1 - Ge + Gr (f3); 2 – PA + 0.1% UNT2 (f6); 3 – PVA + UNT1 (f7); 4 – PVA + UNT2 (f9)

The weak absorption bands observed in the spectra may have different origin. The resonance light absorption in the

near UV region may be generated by electron transitions. The molecules of Ge correspond in fact to fibrillar protein containing peptide groups $>NH\cdots O=C<$ with a hydrogen binding. These groups feature electron transitions of the type $n-\pi^*$ absorbing at $\lambda > 200$ nm. The absence of such bands in PA spectra whose molecules also contain $>NH\cdots O=C<$ groups may be due to a very low intensity of the transition that depends upon the structure and composition of the molecule and its environment.

As for the PVA films, the appearance of the absorption band in the UV region can be explained by rupture of hydrogen bonds (Cang, 1980).

The attainment of a more homogeneous transmittance of PVA and Ge films in contrast to PA in the region 350÷800 nm is of great practical importance (neutral filters). The introduction of low concentrations of carbon fillers (≤ 1 mass%) does not practically reduce the uniformity ratio (Fig. 1b), whereas the transmittance may be varied within the needed limits by changing concentration of the particles and film thickness.

We have found out earlier (Kovalevskaya et al., 2006) that with particle concentration $C \geq 0.1$ mass% in the PA +UNT2 films the dependence of the light attenuation factor on the particle concentration ceases to be linear and the Bourger-Lambert-Beer law is no longer observed. The violation of this law is caused in this case by integration of solid particles in the films into a 3D fractal cluster (Smirnov, 1986). The transparency of the films can be determined when recording spectrum $T(\lambda)$ by this fractal projection onto the plane.

UNT2 particles look like cylindrical tubes of R radius and l length. They are arranged at random angles so that the mean area of the tube projection on the plane is $S_f = 0.5\pi l/R$. The fractal cluster starts growing with increasing amount of the particles. To describe the fractal structure, we take the cluster-cluster model of growth as most appropriate in our case, since the miniclusters are initially formed, which further merge with each other. The mean particle density in this cluster ρ falls with stretching from the center following the law (Smirnov, 1986):

$$\rho(r) = const / r^\alpha, \quad (1)$$

where r – distance from the center ($R_f \gg r \gg R$; R_f – cluster dimensions), $\alpha = d_n - d_f$; d_n – dimensionality of space (1, 2, 3), d_f – fractal dimension ($\alpha \approx 1.5$ in our case).

According to Bourger's law, the intensity of light having passed in direction z through the film is proportional to $\exp(-e \cdot u)$, where e – light attenuation ratio, u – optical thickness of the cluster in a given direction z (Smirnov, 1986):

$$u = \int_{-\infty}^{+\infty} \frac{dS_f}{dV_f} dz = \int_{-\infty}^{+\infty} \frac{\pi}{2} a \frac{dL_f}{dV_f} dz, \quad (2)$$

where dL_f – total length of nanotubes in element dV_f .

We may write for the mass of nanotubes in element dV_f :

$$dM_f = \rho dV_f = \rho_{nm} \pi a^2 dL_f, \quad (3)$$

where ρ – mean density of the composite film in element dV_f , ρ_{nt} – mean density of UNT material.

Let us denote the distance from the cluster center to the beam line ($b \ll R$) as b . Hence, with account of directions 1, 2, 3, we may write

$$u = b\rho(b) \int_{-\infty}^{+\infty} \frac{\rho(z)dz}{2a\rho_{um}} \quad (4)$$

In the case of low concentration of the nanotubes and small thickness of the films, it seems expedient to consider the integral within the limits ($\pm r$):

$$u \approx \frac{b\rho(b)}{2a\rho_{um}} \int_{-r}^{+r} z^{-1.5} dz \approx \frac{b\rho(b)}{a\rho_{um}} \left(-\frac{z^{-0.5}}{0.5} \Big|_{-r}^r \right) \approx \frac{b}{a} \rho(b) \left(-\frac{1}{\sqrt{r}} + 1 \right) \quad (5)$$

As far as $r \gg a$, then we shall obtain that $u \approx 1$ at $a = 1$, $r = 100$, $b = a$, $\rho_{nt} \approx 1$.

With increasing b the value of u will diminish, while the cluster transparency will increase. As the concentration of nanotubes increases the number of original nanoclusters grows, so in the absence of their center ordering, the fractal will turn opaque (we may anticipate that forced orientation of the particles using light, electric or hydrodynamic fields will assist in creation of regular semitransparent structures like optical networks or lattices). This fractal may grow in provision that the particle-particle attraction forces dominate or otherwise, some other cluster type will start growing in which the particles will be embedded into the cluster of the matrix or interfacial zone.

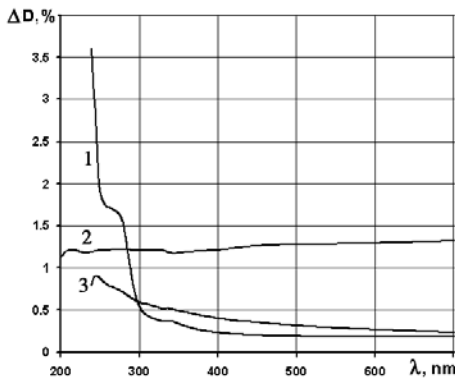


Fig. 2. Difference spectra of optical density $\Delta D(\lambda)$ for unfilled and filled films: 1 – (Ge + Gr) – Ge; 2 – (PVA + UNT2) – PVA; 3 – (PA + 0.5 mass% UNT2) – PA

The weak absorption zone observed in the spectra of the composites based on PVA and Ge in the near UV region are of specific scientific interest due to the probability of obtaining new data on the electron properties of carbon nanoparticles. Proceeding from Ajayan et al. (2003), graphite is a semimetal, while nanotubes are metallic or semiconducting. In the presence of free electrons and low particle concentration, a distinctive absorptive band may appear in the spectra, which is intrinsic for certain metals (Born and Wolf, 1970; Markel et al., 1991). To verify this assumption, we have obtained the spectra of difference

in optical density $\Delta D(\lambda)$ of the filled and unfilled films. Most typical of the spectra are illustrated in Fig. 2. The figure shows that the spectrum of difference of PA-based films is in the form of a weak asymmetrical absorption band with a broadening in the long wavelength and a maximum about 250 nm.

This is just the form that the absorption band should have for spherical metal nanoparticles in a rarified fractal (Markel et al., 1991). Nevertheless, spectrum $\Delta D(\lambda)$ of the films based on PVA is devoid of named peculiarities, although the concentration of nanotubes in them is higher than in PA. Spectrum $\Delta D(\lambda)$ for the films Ge + Gr complies fully with that of the matrix. Proceeding from above results, a conclusion has been derived that there are no proper absorption bands in these spectra at low concentrations of carbon micro and nanoparticles. With increasing concentration, the composite films become opaque as a result of light absorption by carbon particles at interfacial electron transitions. The high value of ΔD in the composite films based on Ge is, evidently, due to the incremented absorption in the interfacial region as compared to that in pure Ge ($n-\pi^*$ transition). The increasing intensity can be attributed to a dominating orientation of electron dipoles parallel to the vector of the electric field light wave, which is in our case parallel to the film surface. This orientation occurs in the vicinity of Gr particles. Notice that, there is no such increase in the intensity in the PVA-based films.

3.2. Microstructure of composite films

Immediately after pouring, the aqua dispersion of the mixture is uniformly gray. A darker picture with a honeycomb or dendritic pattern appears on the light background upon drying. This is, probably, because some dominating directions of the flow appear at pouring on the substrate, along which the axes of molecules and nanotubes are orienting. Further on, miniclusters and fractals on their base start to form. The dark pattern is preserved after separation of the films from the substrate. The microimages of these films are illustrated in Fig. 3.

The coarse dark areas (graphite particles or agglomerations of nanoparticles) are spread chaotically over the film, while the finer ones form the structures of dendritic or cellular type. They do not contact each other at low concentrations of the particles (< 0.5 mass%) but form loose dark filaments of different thickness at higher concentrations.

Similar results were obtained in Du et al., (2006). Homogeneity of the films was reached only in the case of dispersion in toluene used after pretreatment of nanotubes by surfactants. The dispersion of nanotubes in water was also homogeneous, although having some particle agglomerates in the films.

Proceeding from above said, inhomogeneous films were obtained in aqua dispersions of PVA, Ge, Gr, UNT1 and UNT2. The filler particles form the agglomerates in these films with a honeycombed or dendritic pattern characteristic for the percolation fractal clusters. The films Pa + UNT2 produced by hot molding following the procedure described elsewhere (Kovalevskaya et al., 2006) are homogeneous and look uniformly gray.

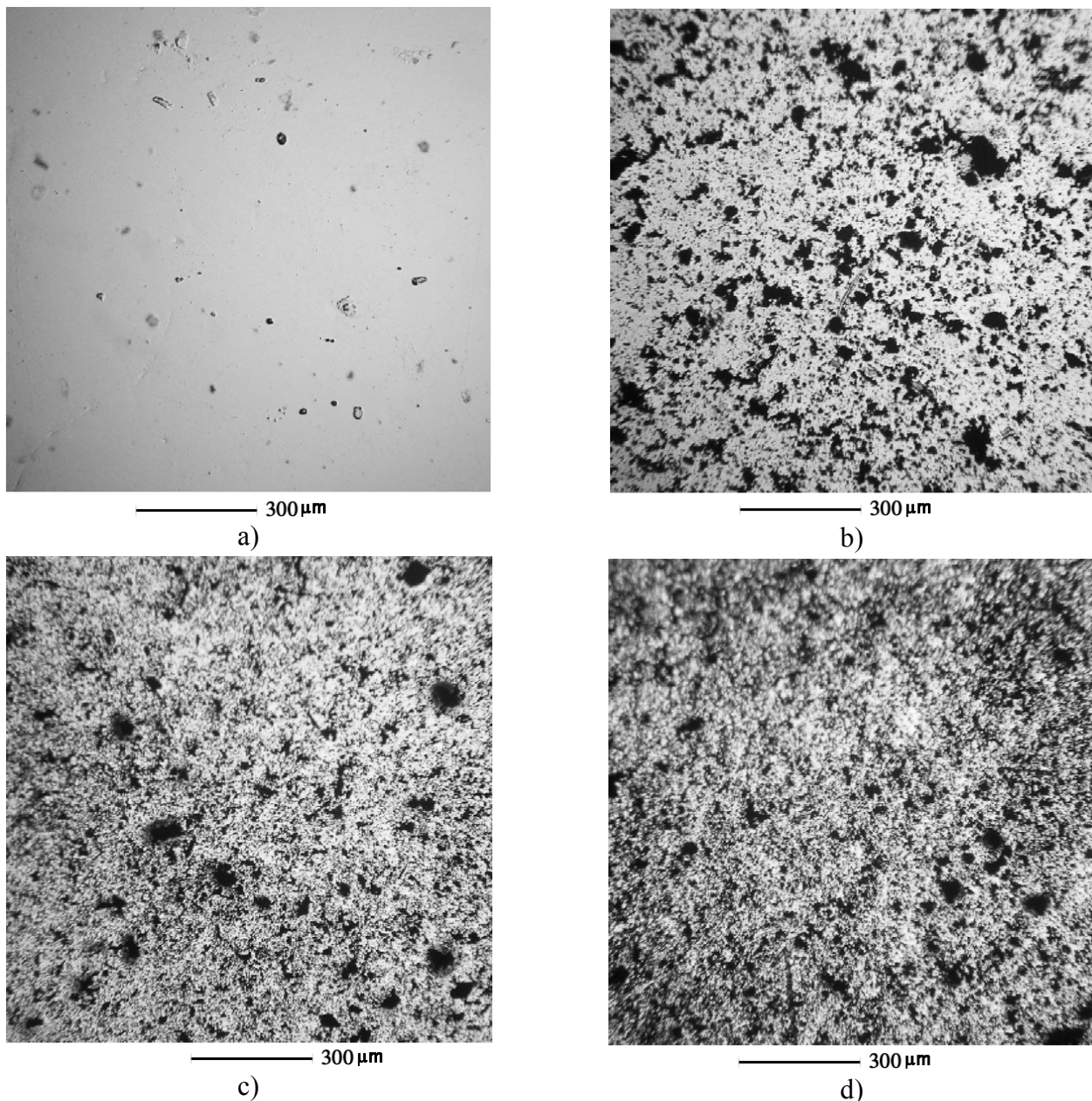


Fig. 3. Optical images of films at 100x magnification: a) Ge on Si (f2); b) PVA + Gr on glass (f4); c) PVA + UNT1 (f7); d) PA + 0.1% UNT2 (f6)

3.3. Supermolecular structure of composite films

Structural parameters of the films derived by processing roentgenograms (Fig. 4) using the standard methods (Wonderlikh, 1976; Martynov and Vylegzhanina, 1972) are presented in Table 2, where d – distance between reflection planes L – crystallite size, Θ – Bragg's angle.

It follows from the results presented in the Table that, first of all, crystallinity degree of the films ω_c , all other conditions being equal, depends only on the type of the substrate (Si – crystalline, glass – amorphous) and carbon particles used.

Let us consider in more detail the mechanism of the substrate effect. The linear polymers are known to easily undergo orientation under the effect of the substrate (specific type of epitaxy) (Wonderlikh, 1976). The macromolecular chain structure promotes packing of their axes

parallel to the substrate surface. Besides, the periodic arrangement of normal to the surface planes in which atoms (or ions) are contained is of importance.

At epitaxy, the axes of polymeric molecules are usually arranged on NaCl, KCl crystals along the directions of similarly charged ions, thus forming folded lamellas with a long fold ($300 \div 500 \text{ \AA}$) presenting the initial face of the polymeric crystal. The compliance between lattices for PA films on KCl surface (020) is within 3%. The epitaxy on quartz crystals is conditioned by the distance between SiOH surface groups multiple to 2.5 \AA (distance between active at adsorption and chemisorption groups of polymer molecules).

The films were grown on one of the face surfaces of Si monocrystal left in room atmosphere for a long time after orientation, cutting, grinding, mechanical and chemical polishing. In these conditions, an oxide film grows on Si

surface whose porous structure is developed and contains O_2 , H_2O , H^+ , OH^- and some other impurities. Most active in interactions with polymeric macromolecules may be $Si-O^-$ and $Si-OH$ groups. Elevated crystallinity of the films can be attributed to the preserved periodicity of Si atoms in the oxide that is imparted by Si structure. According to work Wonderlikh, (1976), along with the epitaxy with folded chains, there may be also the one with straightened chains. Thickness of the lamellas from the straightened chains may reach ≈ 200 nm, and their packing occurs at different angles.

The contribution of amorphous areas and finer deficient crystals is greater in the films grown on the glass substrates (amorphous halo and reflexes in the region $2\theta = 18 - 22^\circ$). The dimensions of coarse crystals (reflexes 1, 2 in the table) are 165, 200, 245 Å, and the finer ones are 50, 100 Å.

The maximal crystallinity $\omega_c = 0.53$ of PVA films filled by Gr, UNT1 and UNT2 grown on glass show the films with UNT2 nanoparticles. Evidently, more coarse Gr and UNT1 particles whose size exceeds characteristic for PVA crystal dimensions ($25 \div 30$ nm) and their orientation mismatches that of the molecular axis induce the formation of a more amorphous fine-crystalline structure.

Notice that the arrangement of the major reflexes in PA and PVA films (synthetic chain polymer, simplest helix) and Ge (biopolymer, fibrillar protein) coincides. Hence, some interplanar spaces in the elementary crystallite cells of named polymers are similar.

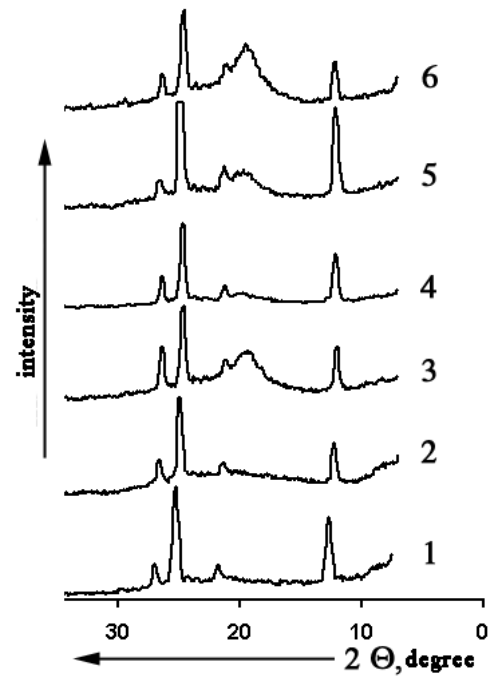


Fig. 4. Radiograms of films: 1 – Ge on Si (f2); 2 – Ge + Gr on Si (f3); 3 – PVA + Gr on glass (f4); 4 – PVA + Gr on Si (f5); 5 – PVA + UNT2 on glass (f6); 6 – PVA + UNT1 on glass (f7)

Tab. 2. Structural parameters of composite films

No	Parameter	Reflex number						ω_c
		1	2	3	4	5	6	
f2	2θ	$26^\circ35'$	$24^\circ48'$	24°	$23^\circ6'$	$21^\circ25'$	$12^\circ26'$	0.57
	$d, [\text{Å}]$	3.35	3.6	3.7	3.86	4.15	7.14	
	$L, [\text{Å}]$	196	244	163	244	121	192	
f3	2θ	$26^\circ35'$	$24^\circ48'$	very weak	-	$21^\circ25'$	$12^\circ26'$	0.27
	$d, [\text{Å}]$	3.35	3.6	3.7	3.86	4.15	7.14	
	$L, [\text{Å}]$	245	244	-	-	162	192	
f4	2θ	$26^\circ35'$	$24^\circ48'$	very weak	very weak	$21^\circ26'$ $19^\circ30'$	$12^\circ26'$	0.42
	$d, [\text{Å}]$	3.35	3.6	3.7	3.86	4.15 4.56	7.14	
	$L, [\text{Å}]$	245	163	-	-	97 48.6	160	
f5	2θ	$26^\circ35'$	$24^\circ55'$	very weak	very weak	$21^\circ26'$ & 3 very weak	$12^\circ26'$	0.62
	$d, [\text{Å}]$	3.35	3.59	-	-	4.15 very weak	7.14	
	$L, [\text{Å}]$	245	244	-	-	162 very weak	192	
f6	2θ	$26^\circ35'$	$24^\circ55'$	-/-	-/-	$21^\circ25'$ & $\sim 19^\circ40'$	$12^\circ26'$	0.53
	$d, [\text{Å}]$	3.35	3.59	-	-	4.15 4.56	7.14	
	$L, [\text{Å}]$	163	195	-	-	121 40	208	
f7	2θ	$26^\circ35'$	$24^\circ55'$	-/-	-/-	$21^\circ25'$ and $\sim 19^\circ40'$	$12^\circ26'$	0.40
	$d, [\text{Å}]$	3.35	3.59	-	-	4.15 4.56	7.14	
	$L, [\text{Å}]$	164	163	-	-	121 37.3	192	

4. SUMMARY

The analysis of the results obtained proves that introduction of low concentrations of carbon particles into the polymeric films based on Ge, PVA and PA ($C = 0.05 \div 0.5$ mass%) makes it possible to regulate transparency of the films in UV and visible spectra within a wide range. Notice that light transmittance in the region $350 \div 800$ nm is practically independent of the wavelength. This property of the particles can be employed in manufacture of neutral filters and glass tinting used for various purposes in engineering.

Carbon particles under study are devoid of their proper absorption bands in UV region, but are able to change the total absorption of the films via increasing or decreasing its intensity at the interface.

When the forces of attraction between particles dominate in the film-forming dispersion, these particles form numerous clusters in the process of film preparation by pouring. These clusters are further joining into a fractal structure. The model of fractal growth suggested by Vitten and Sander (cluster-cluster [9]) is applicable in our case. Density of these fractals diminishes with distance from the center, therefore, transparency of the films is inhomogeneous (Fig. 3). The features of the fractal structure (cellular and dendritic types) depend on the flow direction arising at dispersion pouring onto the substrate and orienting effect of the atomic potential of the substrate (if it is crystalline), as well as particle shape and size. Regular structures similar to lattices or networks can be created by regulating orientation of carbon nanotubes using hydrodynamic or electric and light fields. These structures can find application in optical industry.

The melt-formed PA-based films produced by the methods described in [5] look like gray homogeneous films. The interaction forces between nanotubes and PA macromolecules dominating in these films hamper aggregation of the particles into clusters. In PVA-based films filled by Gr, UNT1 or UNT2 produced by pouring onto glass, the greater crystallinity is shown by the ones with UNT2 filling ($\omega_c = 0.53$, Table 2). Evidently, long and rigid UNT2 particles induce turning of molecular globules and growth of the crystalline areas from the straightened chains of PVA macromolecules forming hydrogen bonds between OH groups of the neighboring molecules. More coarse shapeless Gr and UNT1 particles reduce crystallinity degree characteristic for the unfilled PVA films.

The films produced by pouring aqua dispersions onto the crystalline substrate show higher crystallinity (Tab. 2) due to the effect of epitaxy of polymeric molecules. This phenomenon presents certain scientific and practical interest in elaboration of nanotechnologies for optoelectronic industry.

REFERENCES

1. **Ajayan P. M., Schalder L. S., Braun P. V.** (2003), *Nanocomposite science and technology*, WILEY-VCH, Weinheim.
2. **Born M., Volf E.** (1970), *Fundamentals of optics*, Nauka, USSR.
3. **Cang R.** (1980), *Physical chemistry with application to biological systems*, Mir, USSR
4. **Du F., Fischer I. E., Winey K. J.** (2006), Interfacial in situ polymerization of single wall carbon nanotube/nylon 6,6 nanocomposites, *Polymer*, Vol. 47, 2381 – 2388
5. **Harris P.** (2003), *Carbon nanotubes and affine structures. Nanomaterials of the 21st century*, Tekhnosfera, Russia.
6. **Kovalevskaya T. I., Ihnatouski M. I., Sviridenok A. I.** (2006), Investigation of optical properties of polyamide films filled by carbon nanotubes, *Materials, Technologies, Tools*, Vol. 11, No. 2, 44 – 48.
7. **Kovalevskaya T. I., Ihnatouski M. I., Sviridenok A. I., Voina V. V.** (2007), Peculiarities of interactions between soft X-ray radiation and polyamide films filled by carbon nanotubes, *Materials, Technologies, Tools*, Vol. 12, No. 1, 45–50.
8. **Markel V. A., Muratov L. S., Stockman M. I., George T. F.** (1991), Theory and numerical simulation of optical properties of fractal clusters, *Physical Review*, Vol. 43, No. 10, 8183 – 8187.
9. **Martynov M. A., Vylegzhanina K. A.** (1972), *Radiography of polymers*, Khimiya, USSR.
10. **Pool-jr, Owens F.** (2006), *Nanotechnologies*, Tekhnosfera, Russia.
11. **Smirnov B. M.** (1986), Fractal clusters, *Successes in Physical Sciences*, Vol. 149, Issue 2, 178 – 191
12. **Takasaki T., Kuwana Y** (2000), Polymer Science, *Polymer Chemistry*, Vol. 38, Issue S1, 4832 – 4838.
13. **Wonderlich B.** (1976), *Physics of Macromolecules*, Mir, Russia.